Chaos
An Interdisciplinary Journal of Nonlinear Science

RESEARCH ARTICLE | MAY 12 2026

Thermodynamics of driven systems via the Kuramoto–Sivashinsky equation

E. Hansen ; W. Barham ; P. J. Morrison

Chaos 36, 053127 (2026)
https://doi.org/10.1063/5.0326280

Thermodynamics of driven systems via the Kuramoto–Sivashinsky equation

Cite as: Chaos 36, 053127 (2026); doi: 10.1063/5.0326280
Submitted: 4 February 2026 · Accepted: 24 April 2026 ·
Published Online: 12 May 2026

E. Hansen,[1,a)] W. Barham,[2] and P. J. Morrison[1,b)]

AFFILIATIONS

[1]Institute of Fusion Studies, University of Texas at Austin, Austin, TX, 78712, United States of America
[2]Theoretical Division, Los Alamos National Laboratory, Los Alamos, NM, 87545, United States of America

[a)]**Author to whom correspondence should be addressed:** ehansen99@utexas.edu
[b)]**URL:** https://web2.ph.utexas.edu/morrison/

ABSTRACT

We examine the differences between the driven turbulence described by the Kuramoto–Sivashinsky (KS) equation and the second law of thermodynamics. A general velocity and entropy density system is analyzed with the unified thermodynamic algorithm of metriplectic dynamics, and we show that the positive spectra of the KS equation due to an external energy source prevent its metriplectic description. A variant of the KS equation is produced that monotonically generates an entropy, but the only equilibria of this variant system are spatially constant. Numerical experiments are performed comparing the evolution of the KS equation and its thermodynamic variant. The entropy of this thermodynamic system is increased further by the driving effects of the KS equation, reconciling the generation of entropy with the energy source of the KS equation. Further numerical experiments restrict the positive spectra in the KS equation to determine the effect on the system time evolution. While rescaling the growth rates of instabilities reproduces similar behavior on a slower time scale, introduction of individual positive spectra reproduces the formation of equilibria, relative equilibria, and a transition to chaos. The unified thermodynamic algorithm's implications for the KS equation and the transition between the KS equation and its metriplectic counterpart present a novel pathway to study deterministic dynamical systems with instability.

The Kuramoto–Sivashinsky (KS) equation is a simple model equation containing an energy source, energy dissipation, and nonlinear advection. But we question how the emergence of chaos in this system is consistent with the universal increase of entropy required by thermodynamics. In fact, we show that under thermodynamically consistent dynamics, otherwise chaotic trajectories of the KS equation decay to constant values. However, an entropy designed with the metriplectic framework increases further when forcing is present, reestablishing consistency with universal entropy gain. When the number of instabilities in the system is restricted, we find a variety of stationary states, traveling waves, and chaotic solutions, showing strong sensitivity to how energy is injected in a turbulent system.

I. INTRODUCTION

The second law of thermodynamics is commonly associated with the universal increase of disorder. In a fluid context, this is interpreted as the uniform distribution of fluid properties.[1] But many examples of physical systems exist where patterns emerge spontaneously and nontrivial solutions form. We mention four such examples here. In the study of thermal combustion, flame fronts exhibit complicated motion. Wrinkles form through the interaction of thermal expansion and diffusion, and their amplitude is limited by turbulence in the gas.[2] In the study of plasmas in fusion reactors, an instability known as the trapped ion mode develops spontaneously and has major implications for plasma confinement. Steady states of the trapped ion mode appear as oscillations that are excited by ion–electron collisions and depleted by the process of Landau damping.[3] In the study of thin films flowing down an inclined plane, wavy patterns form due to a competition of gravitational acceleration and viscous dissipation.[4–6] In the study of chemical turbulence and reaction diffusion systems, certain reaction equilibria are given energy by diffusion, and higher order viscous damping allows the formation of a stable pattern.[7] In each of these examples, we observe a competition between the dissipation expected from the second law of thermodynamics and mechanisms that cause oscillations to grow.

We seek an understanding of how the entropy develops in a setting where we see the formation of patterns.

Model systems describing each of the above examples have been analyzed asymptotically by separating long and short wavelength behavior. In all cases, this leads to the same reduced model, the Kuramoto–Sivashinksy (KS) equation,[8]

$$\frac{\partial v}{\partial t} + vv_x = -v_{xx} - vv_{xxxx}, \quad 0 \le x \le L. \tag{1}$$

Here, $v(x, t)$ is a dependent variable depending on the position x in the spatial domain and time t. We assume all quantities in Eq. (1) are unitless in some scale of interest. In the case of combustion, $v(x, t)$ defines the gradient of a perturbation to a flame front surface. In the case of the trapped ion mode, v represents a scaled electric potential. In the case of thin films, v represents the stream function. In the case of chemical turbulence, v represents the gradient of the amplitude phase.

Throughout this study, we consider solutions $v(x) \in L^2([0, L])$ with periodic boundary conditions, spanned by the Fourier basis $\{e^{2\pi ik/L}\}$. For this space, the KS equation with periodic boundary conditions admits unique solutions.[9]

The KS equation has several properties that make it a useful model of driven turbulence. It is invariant under the reflection operator $Rv(L/2+x) = -v(L/2-x)$, which causes solutions that begin antisymmetric to remain antisymmetric for all times.[10] The KS equation is able to account for instabilities through the second derivative term and dissipation through the hyperviscosity term, v_{xxxx}. A balance of these terms coupled with the nonlinear convective derivative defines the behavior of the system. Periodic, wavelike behavior and continuous, oscillatory shocks (as termed by Hooper and Grimshaw) are well documented.[11–13] As the parameter $\tilde{L} = \frac{L}{2\pi\sqrt{\nu}}$ increases, the wavelength of stationary standing waves decreases and traveling waves emerge;[14] this number corresponds to the number of linearly unstable solutions.[8] The fact that many Fourier modes are dissipated has allowed estimates of the dimension of strange attractors for the KS system.[15] This dissipation allows the dynamics of the Kuramoto–Sivashinsky equation to tend toward a finite-dimensional inertial manifold, as initially showed for Neumann boundary conditions and generalized to all initial data.[16,17] Thus, the KS equation exhibits a wide variety of behavior required of systems with both forcing and dissipation, allowing the equation to serve as a useful model of driven turbulence.

Interactions between gradient dissipative dynamics and Hamiltonian dynamics are well known to play an important role in the rate thermodynamics of mesoscopic media.[18] For example, while a local Maxwellian distribution function of a gas may pause the increase in entropy, its instability under hydrodynamic flow creates a large rate of entropy production.[19,20] Here, we examine how the nonlinear dynamics and pattern formation modeled by the KS equation are consistent with the growth of universal entropy. This may be accomplished with the metriplectic formalism, which describes systems that satisfy the first and second laws of thermodynamics.[21–23] Specifically, metriplectic systems use a symmetric bracket (which implies a degenerate gradient flow) to add dissipative terms to an energy-conserving, Hamiltonian description. The dissipation monotonically generates some quantity conserved by the Hamiltonian dynamics, thus turning a thermodynamically reversible system into an irreversible one. The recent unified thermodynamic (UT) algorithm uses the principles of nonequilibrium thermodynamics to provide choices of bivectors for a particular system that construct this symmetric bracket. Several systems have been equipped with a metriplectic bracket in this way, including the Navier–Stokes–Fourier system of a fluid with heat conduction.[24,25] When the dissipative and forcing higher derivatives are removed, the KS equation matches Burgers' and the 1D Navier–Stokes equations and hence satisfies the first law of thermodynamics in the same way. With this similarity to a metriplectic fluid system, we question whether we can use the UT algorithm to find the generated entropy we need for the KS equation.

As we will show, the answer is negative precisely because of the driving that causes the presence of instability. However, due to the small scale dissipation of the KS system, it is possible to build an entropy for a metriplectic KS equation, which only includes dissipation. We then perform a series of numerical experiments with this metriplectic KS system. The body of literature around the KS equation is vast and provides many examples of steady and traveling solutions, the formation of chaos from wave interactions, and energy generation and depletion. These examples are tested in the metriplectic KS system to determine what if any chaotic behavior is retained. We may also use the evolution of the KS equation to determine what would happen to the positive-definite metriplectic entropy if unstable modes are driven. The modifications removing unstable modes also inspire a new approach to varying instabilities of the KS equation, and we test what solutions form when all positive spectra vary in amplitude or only certain modes are retained.

II. METRIPLECTIC STRUCTURE OF THE KS EQUATION

As mentioned earlier, the UT algorithm relates the dissipative dynamics of a metriplectic system to the thermodynamic fluxes J^α and forces Z_α of that system. Consider a system with velocity v and entropy density σ. The UT algorithm then prescribes the dynamics of the system as[25]

$$\begin{aligned} \frac{\partial v}{\partial t} - \{v, H\} &= \mathcal{L}^v(J^v), \\ \frac{\partial \sigma}{\partial t} - \{\sigma, H\} &= \mathcal{L}^\sigma(J^\sigma) + Z_\alpha \tilde{L}^{\alpha\beta} Z_\beta, \end{aligned} \tag{2}$$

where {,} is a Poisson bracket,

$$H = \int_0^L \left(\frac{1}{2}v^2 + \sigma T\right) dx \tag{3}$$

is the total energy of the system,[26] $\tilde{L}^{\alpha\beta}$ is a tensor of the phenomenological coefficients defining the system dissipative dynamics, and $\mathcal{L}^\alpha$ is a pseudodifferential operator. For our purposes, we ascribe no physical meaning to the temperature T corresponding to the KS equation and scale it out as $T = 1$. Below the symbol $H_\alpha = \delta H/\delta\alpha$ is the functional derivative of H with respect to the field α. If the forces and fluxes are taken as

$$Z_\alpha = \mathcal{L}^\alpha_* H_\alpha \quad \text{and} \quad J^\alpha = -H_\sigma \tilde{L}^{\alpha\beta} Z_\beta, \tag{4}$$

with $\mathcal{L}^\alpha_*$ being the dual of the operator $\mathcal{L}^\alpha$, the total energy of the system will be conserved.[25] The UT algorithm defines a metriplectic

bracket of the system as the Kulkarni–Nomizu product[23]

$$\int_0^L \Sigma(dF, dG)M(dK, dN) + \Sigma(dK, dN)M(dF, dG) - \Sigma(dF, dN)M(dG, dK) - \Sigma(dG, dK)M(dF, dN)\, dx \tag{5}$$

of the bivectors

$$\Sigma(dF, dG) = \left(\mathcal{L}_*^{\alpha} F_{\alpha}\right) \tilde{L}^{\alpha\beta} \left(\mathcal{L}_*^{\beta} G_{\beta}\right), \qquad M(dF, dG) = F_{\sigma} G_{\sigma}. \tag{6}$$

In what follows, we will attempt to define an entropy such that the KS equation coupled with that entropy is a metriplectic system. We want to recover entropy advection, so we modify the Burgers' equation Lie–Poisson bracket to[26]

$$\{F, G\} = \int_0^L -\frac{1}{3} v(F_v \partial_x G_v - G_v \partial_x F_v) - \sigma\left(F_v \partial_x G_{\sigma} - G_v \partial_x F_{\sigma}\right) dx. \tag{7}$$

Notice that the total entropy $S = \int_0^L \sigma\, dx$ satisfies $\{F, S\} = 0$ for an arbitrary functional F, as S is required by the metriplectic formalism to be a Casimir invariant.[23] Aside from the entropy advection, we do not want to modify any dynamics of the KS equation, so we take the phenomenological coefficients to be zero with the exception of $\tilde{L}^{vv}$. Then, the UT algorithm gives a system

$$\frac{\partial v}{\partial t} + v v_x = -\mathcal{L}^v\left(\tilde{L}^{vv} \mathcal{L}_*^v(v)\right), \qquad \frac{\partial \sigma}{\partial t} + \partial_x(\sigma v) = \tilde{L}^{vv}\left(\mathcal{L}_*^v(v)\right)^2. \tag{8}$$

This allows a one-way coupling from the velocity of the KS equation into an entropy.

We observe that the operator on the right hand side of the velocity equation in Eq. (8) has a negative spectrum under the assumption $\tilde{L}^{vv} > 0$ since $\mathcal{L}^v \mathcal{L}_*^v$ is positive for an arbitrary choice of the pseudodifferential operator. However, the operator

$$T_{KS} \equiv -\partial_{xx} - \nu \partial_{xxxx} \tag{9}$$

has a positive element of its spectrum. This is easily verified because

$$T_{KS}\, e^{2\pi i k x/L} = g(k)\, e^{2\pi i k x/L}, \qquad \text{where} \quad g(k) = \left(\frac{2\pi k}{L}\right)^2 - \nu\left(\frac{2\pi k}{L}\right)^4 \tag{10}$$

and $g(k) \geq 0$ when $k \leq \frac{L}{2\pi\sqrt{\nu}} = \tilde{L}$. This demonstrates that the instabilities of the KS equation for long wavelengths prevent the definition of an entropy through the UT algorithm.

In order to maintain a thermodynamically consistent component of the KS equation, we see that we will have to remove the unstable modes of the system. If we write a velocity profile as

$$v(x) = \sum_{k=-\infty}^{\infty} v_k\, e^{2\pi i k x/L}$$

in terms of its Fourier components v_k, the result of applying the operator T_{KS} to $v(x)$ is given by

$$T_{KS} v(x) = \sum_{k=-\infty}^{\infty} g(k) v_k\, e^{2\pi i k x/L}. \tag{11}$$

To exclude instabilities from the KS system, we restrict the effect of T_{KS} to modes which are depleted, defining a filtered dissipation operator

$$T_{diss} v(x) = \sum_{k=-\infty}^{\infty} g(k)\Theta(|k| - \tilde{L}) v_k\, e^{2\pi i k x/L}, \tag{12}$$

where $\Theta(|k| - \tilde{L})$ is the Heaviside theta function that only assumes a nonzero value when $|k| \geq \tilde{L}$. This operator only has nonpositive spectra, so it is consistent with the form required by the UT algorithm. In fact, writing $T_{diss} = -\mathcal{L}^v \mathcal{L}_*^v$, we may even write down $\mathcal{L}^v$ by calculating its square root using the Fourier basis

$$\mathcal{L}^v v(x) = \sum_{k=-\infty}^{\infty} \sqrt{-g(k)}\Theta(|k| - \tilde{L}) v_k\, e^{2\pi i k x/L}. \tag{13}$$

Notice that $\mathcal{L}^v = \mathcal{L}_*^v$ is self-adjoint. By using T_{diss} and $\mathcal{L}^v$ as new differential operators for our system, we may extract a thermodynamically consistent reduction of the KS equation,

$$\frac{\partial v}{\partial t} + v v_x = T_{diss} v, \tag{14}$$

$$\frac{\partial \sigma}{\partial t} + \partial_x(\sigma v) = (\mathcal{L}^v v)^2. \tag{15}$$

Given that we are mainly interested in the development of global entropy $S = \int_0^L \sigma\, dx$, we integrate Eq. (15) over the spatial domain to find

$$\frac{\partial S}{\partial t} = \int_0^L (\mathcal{L}^v v)^2\, dx, \tag{16}$$

which is the rate of total entropy production.

We conclude this section with a diversion to an alternative perspective on how the KS equation conflicts with the metriplectic viewpoint. It is possible to obtain a symmetric bracket that recovers the behavior of the KS system. To do this, we may compute the Kulkarni–Nomizu product of the bivectors

$$M(dF, dG) = F_{\sigma} G_{\sigma} \tag{17}$$

and

$$\Sigma(dF, dG) = -\frac{\partial F_v}{\partial x}\frac{\partial G_v}{\partial x} + \nu \frac{\partial^2 F_v}{\partial x^2}\frac{\partial^2 G_v}{\partial x^2}, \tag{18}$$

which leads to equations for the velocity and entropy

$$\frac{\partial v}{\partial t} + v v_x = -v_{xx} - \nu v_{xxxx}, \qquad \frac{\partial \sigma}{\partial t} + \partial_x(\sigma v) = -(v_x)^2 + \nu(v_{xx})^2. \tag{19}$$

This manages to recover the KS equation but notice how the total entropy now behaves as

$$\frac{\partial S}{\partial t} = \int_0^L \nu(v_{xx})^2 - (v_x)^2\, dx, \tag{20}$$

which is no longer strictly nonnegative. This owes to the fact that the bivector Σ is no longer positive definite, as is required for a system that produces entropy.

III. NUMERICAL COMPARISON OF ORIGINAL AND DISSIPATIVE KS SYSTEM

With the metriplectic KS Eq. (14) that we have defined, we now perform a numerical study to determine how solutions to the KS Eq. (1) behave under a thermodynamically consistent system. The definition of T_{diss} and $\mathcal{L}$ using the Fourier basis makes a pseudospectral spatial discretization especially convenient. The vv_x nonlinearity convolution is computed pseudospectrally using the 3/2 dealiasing rule, and FFTs are computed using the SciPy Python package.[27] Due to the stiffness of the KS equation, we use the fourth order exponential time integrator developed by Cox and Matthews and used by Kassam and Trefethen and Cvitanovic *et al.* for studies of the KS equation.[10,28,29] The local truncation error for an exponential method does not scale with stiff eigenvalues, so this method performs well compared to similar methods.

To assess the effects of thermodynamic consistency, we sample a variety of initial conditions to studies of the KS equation that have been previously considered in the literature. These conditions show initial wavelike behavior and interactions before disintegrating into chaos and turbulence. By this, we mean that the motion qualitatively forms large amplitude oscillation in time and space with no clear period. We closely consider the benchmarking initial condition used by Kassam and Trefethen,[29]

$$v(x,0) = \cos\left(\frac{x}{16}\right)\left(1+\sin\left(\frac{x}{16}\right)\right),$$
$$0 \le x \le 32\pi, \quad \nu = 1, \tilde{L} = 16. \tag{21}$$

Another established wave that is absorbed into chaos and a strange attractor is a strange hyperbolic point observed by Hyman, Nicolaenko, and Zareski given by the initial profile,[8]

$$v(x,0) = \frac{-21\sin(12\pi x/\sqrt{253}) - \sin(2\pi x/\sqrt{253})}{\sqrt{253}},$$
$$0 \le x \le 2\pi\sqrt{253}, \quad \nu = 4, \quad \tilde{L} = \sqrt{\frac{253}{4}} \approx 7.95. \tag{22}$$

(In the source paper for this example, the length scale is normalized to 2π, the hyperviscosity $\nu = 4$ chosen from the Sivashinsky derivation of the KS equation, and the bifurcation parameter $\alpha = 4\tilde{L}^2$ is used. This example corresponds to $\alpha = 253$.) We also consider relative equilibrium solutions through a perturbed traveling wave used by Cvitanovic *et al.* and a hyperbolic secant profile that evolves to a traveling wave. The initial condition for the perturbed traveling wave is set up by interpolating the profile TW1 given in Fig. 6(a) of Cvitanovic *et al.* for $L = 22$ and $\nu = 1$ ($\tilde{L} = \frac{11}{\pi} \approx 3.50$).[10] Our resulting initial condition is

$$v(x,0) = \frac{1}{20}\sum_{k=-5}^{5} a_k\, e^{\frac{2\pi k i}{L}}, \tag{23}$$

with $a_0 = 0$, $a_1 = -0.5 + 9.4i$, $a_2 = -7.7 + 0.1i$, $a_3 = -1.9 - 6.1i$, $a_4 = 2.7 - 3.9i$, and $a_5 = 2.2 - 0.4i$. The hyperbolic secant profile is set up as

$$v(x,0) = \operatorname{sech}\left(\frac{x}{L} - \frac{1}{2}\right),$$
$$L = 20\pi, \quad \nu = 4, \quad \tilde{L} = 5. \tag{24}$$

We compare the evolution of these cases in the KS Eq. (1) under the metriplectic system (14) throughout Fig. 1. The benchmarking conditions of Kassam and Trefethen shown in Fig. 1(a) strongly interact and form higher order waves and chaos as time passes. Under the thermodynamically consistent dynamics, these initial conditions just begin to beat before they are depleted in Fig. 1(b). The motion is confined to small wiggles as the profile amplitude shrinks. A perturbed traveling wave solution to the KS equation, which originally circles the domain twice before falling apart in Fig. 1(c), barely starts to move before being dissipated under metriplectic dynamics in Fig. 1(d). Figure 1(e) shows the strange hyperbolic point's late transition to chaos, but it never occurs in the metriplectic system. The motion is depleted on a time scale two orders of magnitude before crisis in Fig. 1(f).

Each of these previously complex solutions decreases to zero over the course of the metriplectic dynamics. The hyperbolic secant profile is slightly different from these cases. Under the dynamics of the KS equation, this profile undergoes chaos and oscillates rapidly until it forms a period four traveling wave in Fig. 1(g). The amplitude of this wave has increased significantly from its initial state. Once the instability of the KS equation has been eliminated, it continues to form a wavelike pattern as it circles the domain in Fig. 1(h), but the amplitude of this oscillation is substantially reduced.

We now show the entropy associated with the metriplectic dynamics in the cases considered in Fig. 2. Having defined the total entropy evolution in terms of $v(x, t)$, we may allow ν to be determined by the original KS equation and produce a positive definite entropy. Our main result focuses on the distinction between this forced system entropy and purely metriplectic dynamics. As required by our method, the metriplectic dynamics show positive definite entropy growth. But we see that in every case, the dynamics of the original KS equation cause the entropy to increase further than the dissipative dynamics alone. In contrast to our expectations, the forcing effects that cause nontrivial patterns to emerge in the KS equation do not decrease the metriplectic entropy. This idea establishes the consistency of pattern formation with the second law of thermodynamics.

IV. EQUILIBRIA OF THE DISSIPATIVE KS EQUATION

We have seen in Sec. III that the complicated dynamics that characterize the KS Eq. (1) are transient in the thermodynamically consistent system (14). Now we question whether it is possible for the metriplectic equation to have another type of stationary

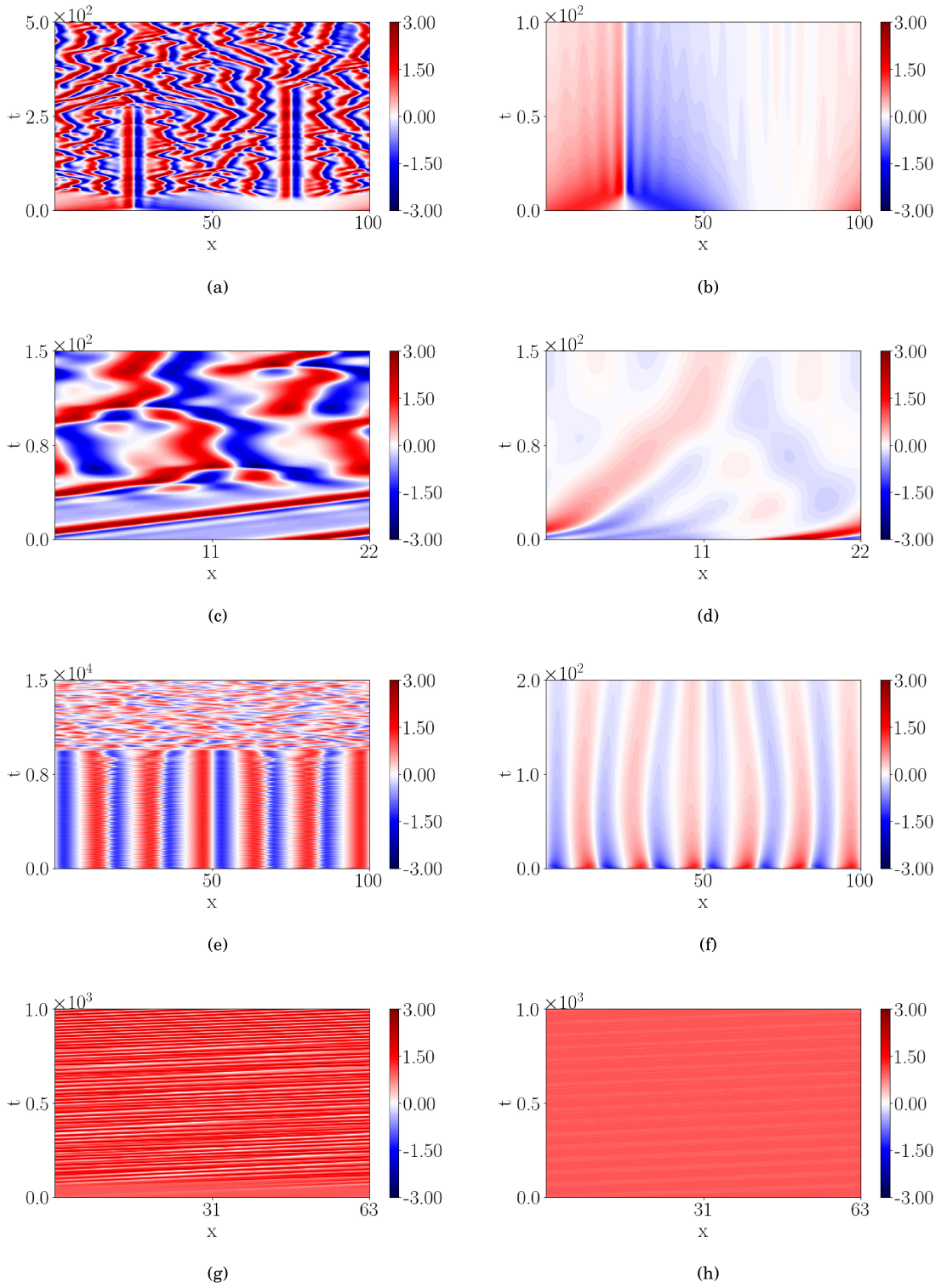

FIG. 1. Solutions of the KS Eq. (1) (left) are dissipated under metriplectic dynamics (14) (right).

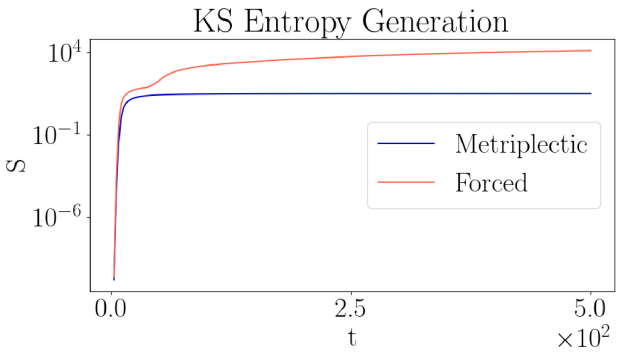

(a) $\cos\left(\frac{x}{16}\right)\left(1+\sin\left(\frac{x}{16}\right)\right)$

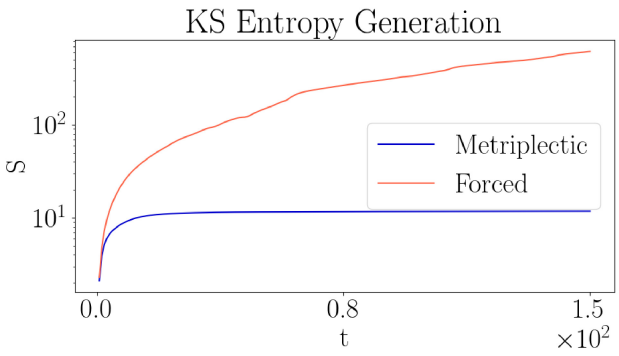

(b) Traveling wave

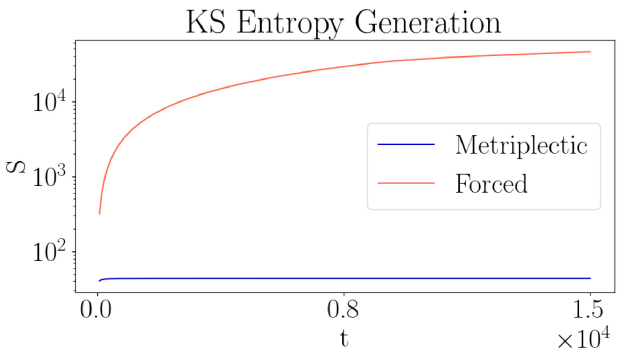

(c) Strange hyperbolic point

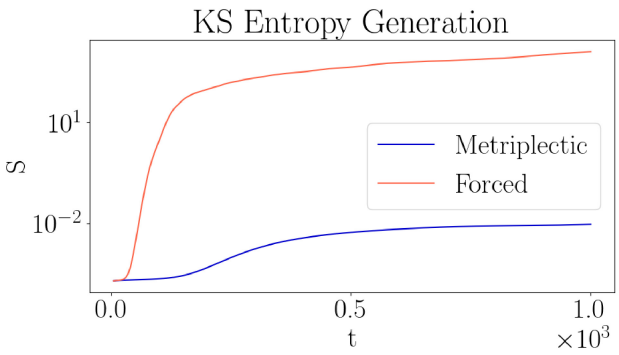

(d) Sech profile

FIG. 2. Generation of entropy (16) as a result of the metriplectic KS Eq. (14) and the fully forced dynamics of the KS Eq. (1) for the initial conditions studied. (a) $\cos\left(\frac{x}{16}\right)\left(1+\sin\left(\frac{x}{16}\right)\right)$. (b) Traveling wave. (c) Strange hyperbolic point. (d) Sech profile.

or periodic solution. Through the method of Lagrange multipliers, equilibria of a metriplectic system that maximize the entropy must satisfy[30]

$$\begin{aligned} \frac{\delta S}{\delta v} - \lambda \frac{\delta H}{\delta v} &= -\lambda v = 0, \\ \frac{\delta S}{\delta \sigma} - \lambda \frac{\delta H}{\delta \sigma} &= 1 - \lambda = 0. \end{aligned} \tag{25}$$

This shows that maximum entropy solutions must satisfy $v=0$. Galilean invariance of the KS equation would suggest that this also allows constant v solutions to have maximum entropy.[10] But equilibria are not required to satisfy this variational principle, and the hyperbolic secant profile mentioned above does not appear to.

To characterize all equilibria of the KS equation, we consider the deviations of solutions to the KS equation with the spatial average value

$$\bar{v} = \frac{1}{L}\int_0^L v(x,t)\,dx. \tag{26}$$

By integrating the KS equation over space, we have

$$\frac{\partial}{\partial t}\int_0^L v\,dx + \int_0^L v v_x\,dx = \int_0^L -\mathcal{L}^v\mathcal{L}^v_* v\,dx \tag{27}$$

or

$$L\frac{\partial \bar{v}}{\partial t} = -\int_0^L \mathcal{L}^v\mathcal{L}^v_* v\,dx - \left[\frac{1}{2}v^2\right]_0^L = 0, \tag{28}$$

as $\mathcal{L}^v\mathcal{L}^v_*$ only acts on high frequency modes that are zero on averaging. This establishes that $\bar{v}$ is constant in space and time. As a result, we may rewrite the KS equation as

$$\frac{\partial (v-\bar{v})}{\partial t} + (v-\bar{v})\partial_x(v-\bar{v}) + \bar{v}\partial_x(v-\bar{v}) = -\mathcal{L}^v\mathcal{L}^v_*(v-\bar{v}). \tag{29}$$

Multiplying by $v - \bar{v}$ and integrating over space yield

$$\frac{\partial}{\partial t}\int_0^L (v-\bar{v})^2\,dx = -\int_0^L (v-\bar{v})\mathcal{L}^v\mathcal{L}_*^v(v-\bar{v})\,dx - \int_0^L ((v-\bar{v})^2 + \bar{v}(v-\bar{v}))\partial_x(v-\bar{v})\,dx = -\int_0^L \left(\mathcal{L}_*^v(v-\bar{v})\right)^2 dx \le 0, \tag{30}$$

where we have integrated by parts and used the fact that the second integral vanishes. With the conservation of $\bar{v}$, this result implies that the metriplectic KS system evolves arbitrary initial conditions to their average value. For a solution to be an equilibrium or periodic in time, the inequality must be saturated with $\mathcal{L}_*^v(v-\bar{v}) = 0$ for all times. But then an equilibrium satisfies

$$vv_x = -\mathcal{L}^v\mathcal{L}_*^v v = 0, \tag{31}$$

and integrating in space yields

$$\frac{1}{2}v(x)^2 = \frac{1}{2}v(0)^2. \tag{32}$$

Thus, we conclude that the only equilibria of the metriplectic KS system are constants.

V. VARIATION OF FORCING STRENGTH

The analysis of the KS Eq. (1) and its metriplectic reduction (14) conducted in Secs. II–IV motivates the study of the instabilities of the KS equation as an external disturbance to a thermodynamically consistent system. We will analyze the effect of the positive spectra on two sets of initial conditions previously mentioned.

These spectra were all removed in the definition of the metriplectic KS system from Secs. II–IV. In order to study the addition of energy injection, we can consider two approaches. In the first, we generalize the KS operator parametrically as

$$T_{KS}^{\epsilon} = -\mathcal{L}^v\mathcal{L}_*^v + \epsilon\left(T_{KS} + \mathcal{L}^v\mathcal{L}_*^v\right), \tag{33}$$

where $T_{KS} + \mathcal{L}\mathcal{L}_*$ represents the positive spectra of the KS antidiffusion and hyperviscosity, as shown, for example, in Fig. 3. The operator T_{KS}^{ϵ} varies continuously between the metriplectic KS Eq. (14) for $\epsilon = 0$ and the KS Eq. (1) for $\epsilon = 1$. One option for reintroducing instability to the metriplectic KS system is to slowly increase ϵ, allowing all positive Fourier coefficients at once albeit with smaller growth rate.

An alternative to this approach would be to drive individual small wavenumbers as subsets of the positive spectra. This alternatively introduces a generalized KS operator as

$$T_{KS}^{I}v(x) = -\mathcal{L}^v\mathcal{L}_*^v v + \sum_{k\in I\cup -I} g(k)v_k\, e^{2\pi ikx/L}, \tag{34}$$

where I is a subset of the unstable wavenumbers $\{1, 2, \ldots, \text{floor}(\tilde{L})\}$. We will primarily focus on the case where I is a singleton containing just one instability, but we also consider cases allowing multiple wavenumbers. Choosing modes allowed in the KS equation allows the study of which combinations of drivers allow certain behavior in the KS system.

The approach of adding forcing components to a Hamiltonian or metriplectic system can be compared with the notion of a port-Hamiltonian (pH) system. A pH system describes the interactions of an otherwise Hamiltonian system with its environment.[31] This is accomplished by means of a Dirac structure and additional pairs of power variables to describe the system boundaries and describes the energy flow through a boundary, external impacts of the Hamiltonian dynamics, and energy dissipation. Irreversible pH systems are also able to account for entropy production by introducing a contact vector field.[32] This is similar to our approach in that it generates entropy and conserves the total energy of the system. However, while the positive spectra in our work correspond to external forcing, they are not interpreted as passing through a spatial boundary of the system.

We perform a numerical study on the Kassam Trefethen initial conditions. As studied, this configuration contains 15 wavenumbers with positive spectra, as shown in Fig. 3(a) [notice $g(\tilde{L}) = 0$]. This allows many subsets of modes to consider to determine how this initial condition transitions to chaos. Under the dynamics of

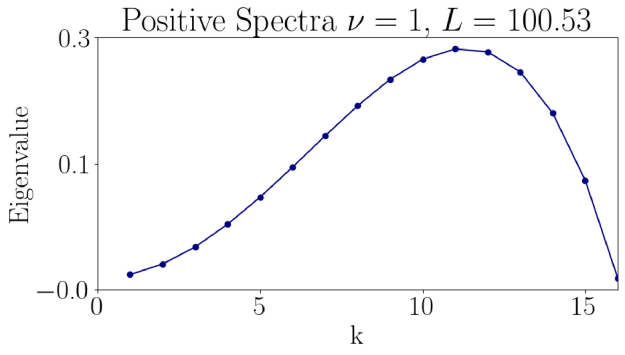

(a) Spectra for $\nu = 1$ and $L = 32\pi$.

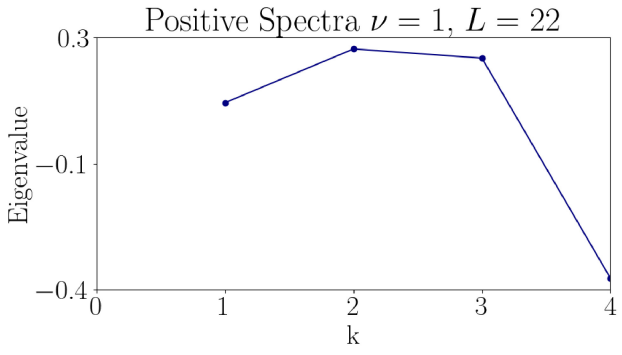

(b) Spectra for $\nu = 1$ and $L = 22$.

FIG. 3. Positive spectra of the Kassam Trefethen benchmarking and TW1 condition parameters of Cvitanovic *et al.*

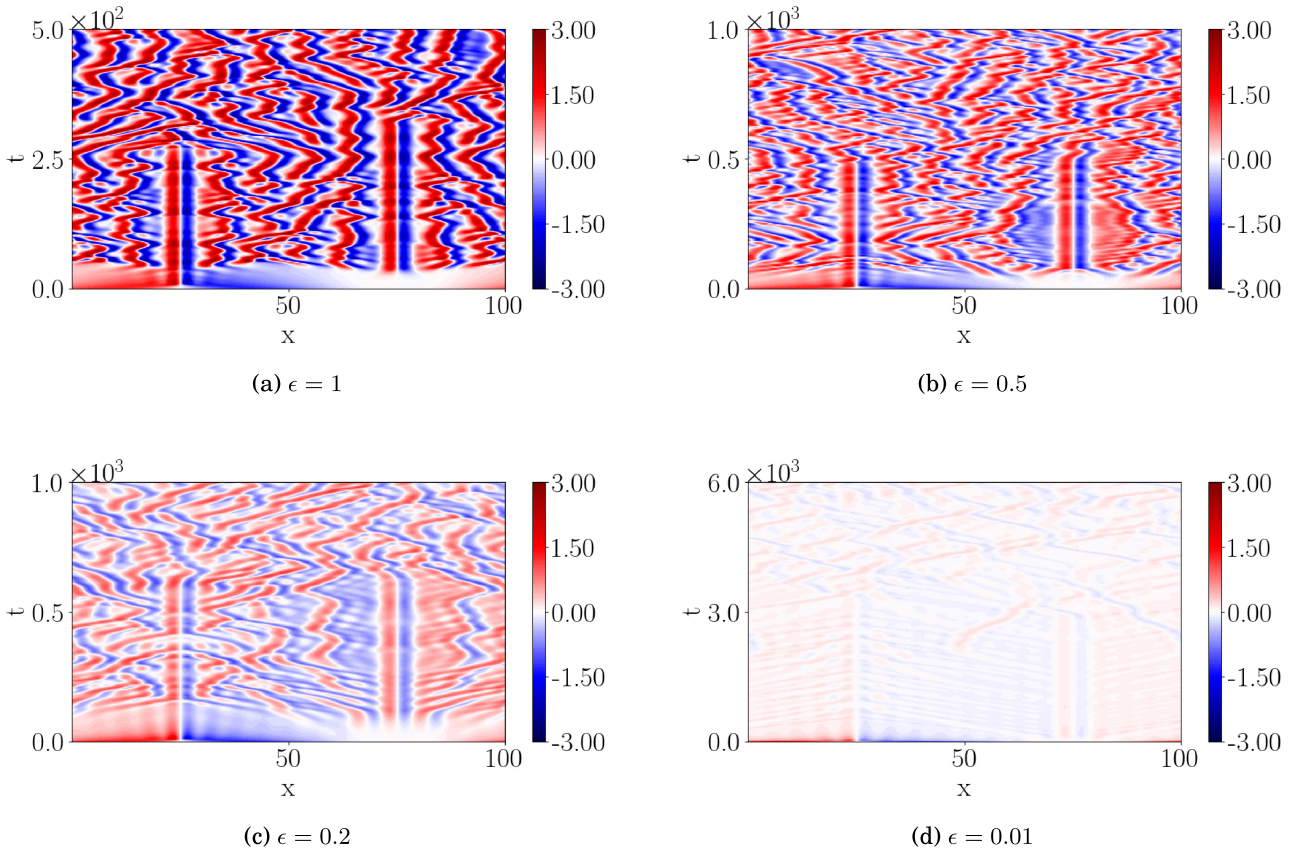

FIG. 4. Spatiotemporal variation of $v(x, t)$ as the growth rate of positive spectra of T^{ϵ}_{KS} is decreased. As the parameter $\epsilon > 0$ decreases, the transition to chaos remains but occurs later in the dynamics, and the amplitude of the oscillations decreases. (a) $\epsilon = 1$. (b) $\epsilon = 0.5$. (c) $\epsilon = 0.2$. (d) $\epsilon = 0.01$.

the unmodified KS equation, Eq. (21) evolves into an ordered pattern of moving waves and transitions into a chaotic attractor at later times. However, the metriplectic system depletes the energy of this mode and only small ripples emerge before they fade away. Consequently, forcing of this system is necessary for nontrivial patterns to be sustained.

We begin by increasing the growth rate of all positive spectra at once. This process is illustrated in Fig. 4; the dynamics of the original KS equation are shown in Fig. 4(a) with $\epsilon = 1$. By decreasing ϵ to half the forcing strength of the original KS equation, we see similar patterns as the motion progresses and the breakdown into the strange attractor from the KS equation. However, we notice that the transition to nonlinear dynamics occurs later. This pattern continues as ϵ decreases to 0.2 and 0.01, suggesting that the presence of all positive spectra is responsible for an eventual transition to chaos regardless of the size of the growth rates.

With this analysis of what occurs when all mode forcings are controlled simultaneously, we consider the effects of injecting individual wavenumbers into the dynamics throughout Fig. 5. We begin by adding the weakest mode corresponding to the first $k = 1$ nonzero wavenumber at which the spectrum assumes a positive value just above zero. At this value, the dynamics are dissipated but achieve a steady state shown in Figs. 6(a) and 6(a). This pattern continues for the fifth positive spectra $k = 5$, where the amplitude of the steady state increases. Equilibria also form when the most unstable modes are driven. When $k = 11$, the mode appears to shake, but the dynamics continue to have frequency 11 for long time scales. A combination of modes $k = 12$ and $k = 13$ also forms an equilibrium. The structure of the resulting steady state appears to follow the period of the driven wavenumber, though small fluctuations appear. In the last case, periodicity of the equilibrium follows the $n = 12$ mode; we might understand this as the stronger growth rate setting the dynamics.

The above injections of one or two positive spectra yielded stable equilibria. However, if we inject the last two instabilities, for example $k = 14$, we see the development of chaos in Fig. 7(a). It is of interest that these modes cause the transition to chaos where the stronger modes $k = 11$ and $k = 12$ did not. Chaos also ensues if we can also inject the first four wavenumbers and find an unstable periodic solution that disintegrates as time progresses, as shown in Fig. 7(b). This is an interesting comparison with the injection of the most unstable mode, where we see an equilibrium that appears

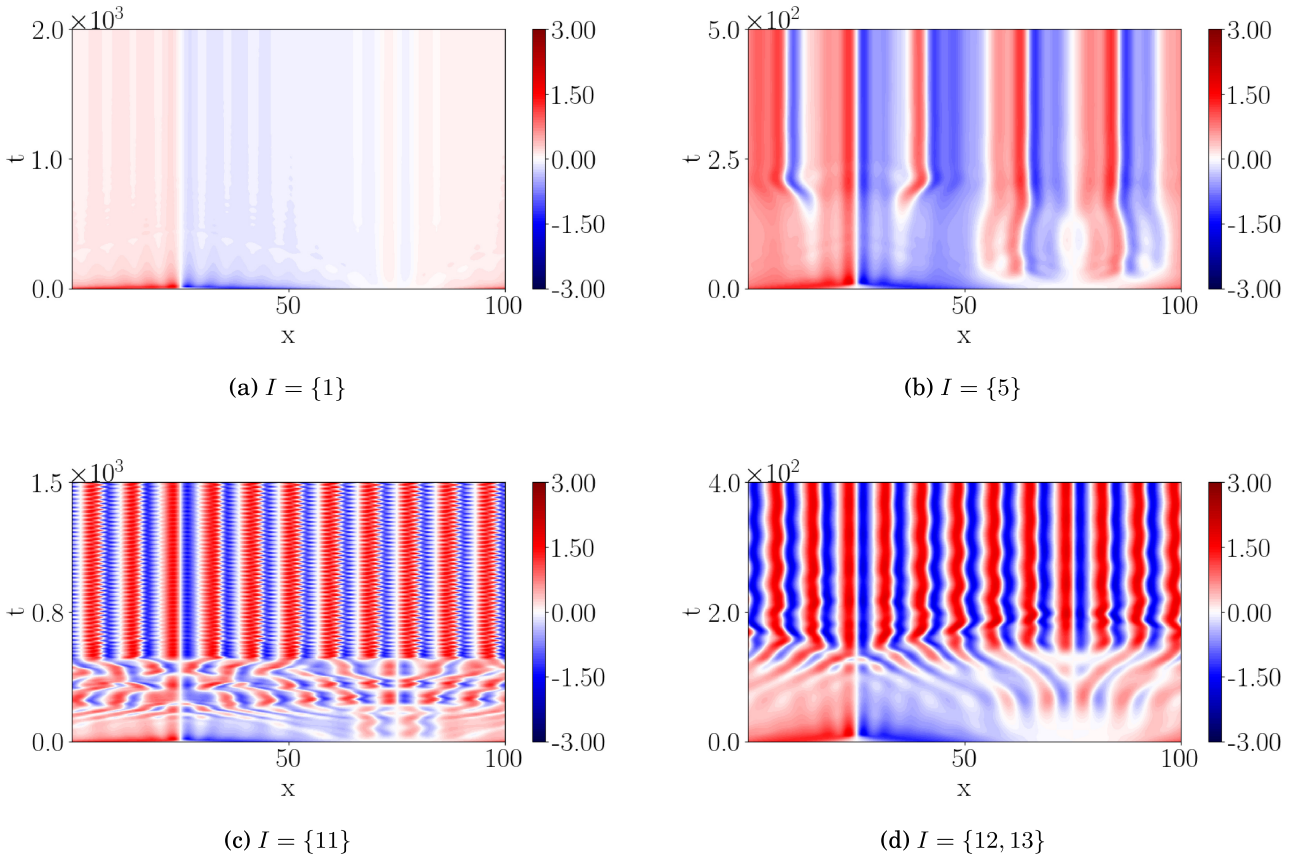

(a) $I = \{1\}$ (b) $I = \{5\}$

(c) $I = \{11\}$ (d) $I = \{12, 13\}$

FIG. 5. Contours of $v(x, t)$ equilibria that form from the Kassam Trefethen initial data with the restriction T^I_{KS} to certain instabilities of the KS equation. (a) $I = \{1\}$. (b) $I = \{5\}$. (c) $I = \{11\}$. (d) $I = \{12, 13\}$.

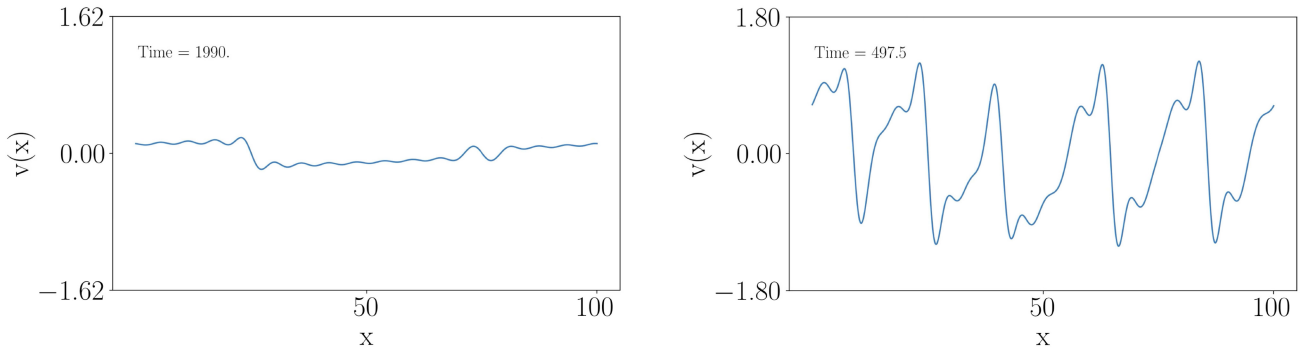

(a) $I = \{1\}$ (b) $I = \{5\}$

FIG. 6. Profiles of equilibria found with T^I_{KS} driven spectra for the Kassam Trefethen initial conditions. (a) $I = \{1\}$. (b) $I = \{5\}$.

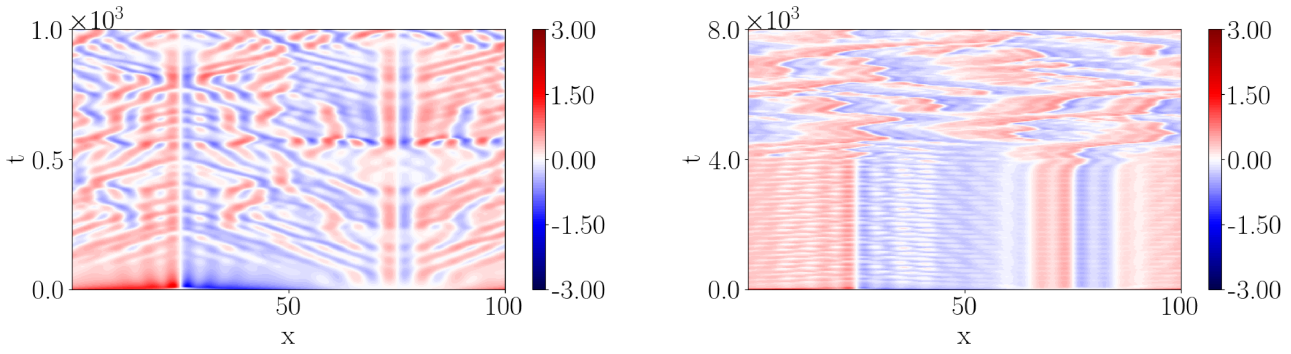

(a) $I = \{14\}$ (b) $I = \{1, 2, 3, 4\}$

FIG. 7. Chaotic solutions resulting from the Kassam Trefethen initial conditions and retention of a subset of KS instabilities in T^I_{KS}. (a) $I = \{14\}$. (b) $I = \{1, 2, 3, 4\}$.

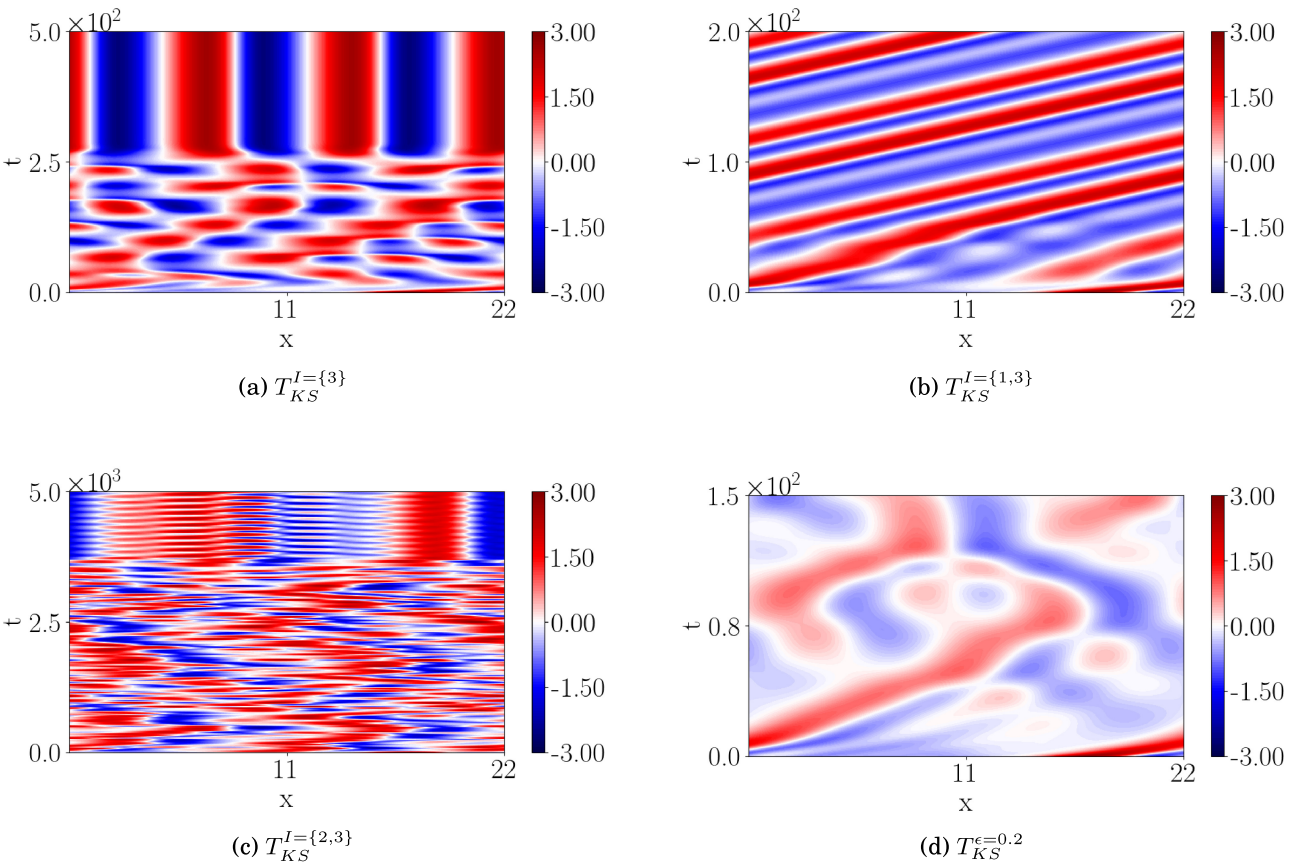

(a) $T_{KS}^{I=\{3\}}$ (b) $T_{KS}^{I=\{1,3\}}$

(c) $T_{KS}^{I=\{2,3\}}$ (d) $T_{KS}^{\epsilon=0.2}$

FIG. 8. Behavior of the perturbed traveling wave solution under alternative forcing T^I_{KS} and T^{ϵ}_{KS}. (a) $T^{I=\{3\}}_{KS}$. (b) $T^{I=\{1,3\}}_{KS}$. (c) $T^{I=\{2,3\}}_{KS}$. (d) $T^{\epsilon=0.2}_{KS}$.

unstable initially but then settles. The contrast here suggests that it is the interactions of instabilities rather than their existence that causes chaos.

Having analyzed various possibilities for forcing this system, we turn to the perturbed traveling wave TW1 of Cvitanovic *et al.* Since this initial condition has a much smaller length scale $L = 22$, there are just three positive spectra to inject into the system, but we still recover nontrivial behavior. When wavenumbers are injected one at a time, we recover an equilibrium, and as an example we show the result of injecting the last unstable wave in Fig. 8(a). This is a commonality with the previous case, except that in this case all modes yield stable equilibria. When we consider combinations of the modes, adding $k = 1$ and $k = 3$ results in a relative equilibrium in Fig. 8(b) that persists for long times without a transition to chaotic behavior. Some chaos is recovered when $k = 2$ and $k = 3$ are injected simultaneously, as shown in Fig. 8(c), but this eventually leads to a periodic orbit. We also see a continued transition to chaos when all unstable spectra are present with a decreased growth rate with the scaling factor $\epsilon = 0.2$. In the $\epsilon = 0.2$ case, we see the traveling wave start to propagate but fall apart without completing a period. There is not enough instability to maintain its dynamics. Going through this example reinforces that the solutions of the KS equation are very sensitive to the energy injection mechanism, so we need just the right forcing to support a given traveling wave or other equilibrium.

VI. DISCUSSION

To analyze the Kuramoto–Sivashinksy equation using the metriplectic framework, we removed all positive spectra caused by the energy injection mechanism. This separation of the forcing and dissipation has accomplished several objectives. We found that chaotic solutions of the KS equation both dissipate and undergo nontrivial behavior under metriplectic dynamics. The entropy prescribed by the UT algorithm increases further when the forcing of the KS equation is present, allowing the consistency of ordered systems with entropy production. Mode filtering showed that unstable behavior from the KS system can simplify to equilibria and relative equilibria when less instabilities are present. Even when all unstable modes are reduced in strength, the eventual transition to chaos remains. Thus, our approach provides a unique perspective both in terms of the metriplectic dynamics and the celebrated dynamical system implications of the KS equation.

This study has separated thermodynamically consistent dissipation mechanisms from linear instabilities forbidden by the UT algorithm. Though we have observed interesting behavior with the entropy we have defined, an entropy based on eliminating unstable modes is inherently artificial. In the decades since the derivations of the KS equation, several of the settings in which it was derived have been shown to be thermodynamically consistent. In particular, the Navier–Stokes–Fourier system is metriplectic, and gravity is a conservative force, so a thin film down a plane is thermodynamically consistent and has an associated entropy.[24,25] Additional systems that have been found to be metriplectic are visco-resistive magnetohydrodynamics[33] and the Vlasov–Maxwell system for two species plasma with the Landau collision operator.[34] This would include electron–ion collisions and Landau damping, key components of the LMRT description of the trapped ion mode.[3] The implications of this work would be supported by a comparison of our entropy metric and the physical entropy of these settings. An alternative asymptotic analysis of the environment leading to the KS equation may lead to a reduced model that retains thermodynamic consistency, creating a truly metriplectic simplified model of turbulence.

ACKNOWLEDGMENTS

This work was supported by U.S. Department of Energy under Grant No. DE-FG02-04ER-54742. W.B. was supported by the Laboratory Directed Research and Development program of Los Alamos National Laboratory under Project No. 20251151PRD1 and Los Alamos Laboratory Report LA-UR-25-32124.

AUTHOR DECLARATIONS

Conflict of Interest

The authors have no conflicts to disclose.

Author Contributions

E. Hansen: Formal analysis (lead); Software (equal); Visualization (lead); Writing – original draft (lead); Writing – review & editing (equal). **W. Barham:** Conceptualization (equal); Formal analysis (supporting); Software (equal); Visualization (supporting); Writing – review & editing (equal). **P. J. Morrison:** Conceptualization (equal); Funding acquisition (lead); Project administration (lead); Supervision (lead); Writing – review & editing (equal).

DATA AVAILABILITY

The data that support the findings of this study are available from the corresponding author upon reasonable request and openly available in GitHub repository, Ref. 35.

REFERENCES

[1] P. K. Kundu, I. M. Cohen, and H. H. Hu, *Fluid Mechanics*, 2nd ed. (Academic Press, San Diego, 2002).
[2] G. I. Sivashinsky, "Nonlinear analysis of hydrodynamic instability in laminar flames—I. Derivation of basic equations," Acta Astronaut. **4**(11), 1177–1206 (1977).
[3] R. E. LaQuey, S. M. Mahajan, P. H. Rutherford, and W. M. Tang, "Nonlinear saturation of the trapped-ion mode," Phys. Rev. Lett. **34**, 391–394 (1975).
[4] D. J. Benney, "Long waves on liquid films," J. Math. Phys. **45**, 150–155 (1966).
[5] G. M. Homsy, "Model equations for wavy viscous film flow," Lect. Appl. Math. **15**, 191–194 (1974).
[6] A. A. Nepomnyashchii, "Stability of wavy conditions in a film flowing down an inclined plane," Fluid Dyn. **9**, 354–359 (1974).
[7] Y. Kuramoto and T. Tsuzuki, "Persistent propagation of concentration waves in dissipative media far from thermal equilibrium," Prog. Theor. Phys. **55**(2), 356–369 (1976).
[8] J. M. Hyman, B. Nicolaenko, and S. Zaleski, "Order and complexity in the Kuramoto-Sivashinsky model of weakly turbulent interfaces," Physica D **23**(1), 265–292 (1986).
[9] B. Nicolaenko and B. Scheurer, "Remarks on the Kuramoto-Sivashinsky equation," Physica D **12**, 391–395 (1984).
[10] P. Cvitanović, R. L. Davidchack, and E. Siminos, "On the state space geometry of the Kuramoto–Sivashinsky flow in a periodic domain," SIAM J. Appl. Dyn. Syst. **9**(1), 1–33 (2010).
[11] U. Frisch, Z. S. She, and O. Thual, "Viscoelastic behaviour of cellular solutions to the Kuramoto-Sivashinsky model," J. Fluid Mech. **168**, 221–240 (1986).

[12]D. Michelson, "Steady solutions of the Kuramoto-Sivashinsky equation," Physica D **19**(1), 89–111 (1986).
[13]A. P. Hooper and R. Grimshaw, "Travelling wave solutions of the Kuramoto-Sivashinsky equation," Wave Motion **10**(5), 405–420 (1988).
[14]J. M. Greene and J.-S. Kim, "The steady states of the Kuramoto-Sivashinsky equation," Physica D **33**(1), 99–120 (1988).
[15]B. Nicolaenko, B. Scheurer, and R. Temam, "Some global dynamical properties of the Kuramoto-Sivashinsky equations: Nonlinear stability and attractors," Physica D **16**(2), 155–183 (1985).
[16]C. Foias, B. Nicolaenko, G. R. Sell, and R. Temam, "Variétés inertielles pour l'équation de Kuramoto-Sivashinski," C. R. Acad. Sci. **301**, 285–288 (1985).
[17]J. C. Robinson, "Inertial manifolds for the Kuramoto-Sivashinsky equation," Phys. Lett. A **184**, 190–193 (1994).
[18]M. Grmela, "Thermodynamics and rate thermodynamics," J. Stat. Phys. **191**, 75 (2024).
[19]H. Grad, "On Boltzmann's H-theorem," J. Soc. Appl. Ind. Math. **13**, 259–277 (1965).
[20]L. Desvillettes and C. Villani, "On the trend to global equilibrium for spatially inhomogeneous kinetic systems: The Boltzmann equation," Invent. Math. **159**, 245–316 (2005).
[21]P. J. Morrison, "Some observations regarding brackets and dissipation," Center for Pure and Applied Mathematics Report PAM-228 (University of California, Berkeley, 1984), arXiv:2403.14698v1[math-ph] (15 March 2024).
[22]P. J. Morrison, "A paradigm for joined Hamiltonian and dissipative systems," Physica D **18**(1), 410–419 (1986).
[23]P. J. Morrison and M. H. Updike, "Inclusive curvaturelike framework for describing dissipation: Metriplectic 4-bracket dynamics," Phys. Rev. E **109**, 045202 (2024).
[24]W. Barham, P. J. Morrison, and A. Zaidni, "A thermodynamically consistent discretization of 1D thermal-fluid models using their metriplectic 4-bracket structure," Commun. Nonlinear Sci. Numer. Simul. **145**, 108683 (2025).
[25]A. Zaidni and P. J. Morrison, "Metriplectic four-bracket algorithm for constructing thermodynamically consistent dynamical systems," Phys. Rev. E **112**, 025101 (2025).
[26]P. J. Morrison, "Hamiltonian description of the ideal fluid," Rev. Mod. Phys. **70**, 467–521 (1998).
[27]C. Canuto, M. Y. Hussaini, A. Quarteroni, and T. A. Zang, *Spectral Methods: Fundamentals in Single Domains*, 1st ed., Scientific Computation (Springer, Berlin, Heidelberg, 2006).
[28]S. M. Cox and P. C. Matthews, "Exponential time differencing for stiff systems," J. Comput. Phys. **176**(2), 430–455 (2002).
[29]A.-K. Kassam and L. N. Trefethen, "Fourth-order time-stepping for stiff PDEs," SIAM J. Sci. Comput. **26**(4), 1214–1233 (2005).
[30]C. Bressan, M. Kraus, O. Maj, and P. J. Morrison, "Metriplectic relaxation to equilibria," arXiv:2506.09787v1[math-ph] (2025).
[31]A. J. van der Schaft and B. M. Maschke, "Hamiltonian formulation of distributed-parameter systems with boundary energy flow," J. Geom. Phys. **42**(1), 166–194 (2002).
[32]D. Eberard, B. M. Maschke, and A. J. van der Schaft, "An extension of Hamiltonian systems to the thermodynamic phase space: Towards a geometry of nonreversible processes," Rep. Math. Phys. **60**(2), 175–198 (2007).
[33]M. Materassi and E. Tassi, "Metriplectic framework for dissipative magnetohydrodynamics," Physica D **241**(6), 729–734 (2012).
[34]M. Kraus and E. Hirvijoki, "Metriplectic integrators for the Landau collision operator," Phys. Plasmas **24**(10), 102311 (2017).
[35]W. Barham and E. Hansen (2026). "KS-metriplectic-analysis," https://github.com/ehansen99/KS-Metriplectic-Analysis